SPECTRAL EVOLUTION OF SWELL ACROSS THE CONTINENTAL SHELF

Fabrice Ardhuin[1], W.C. O'Reilly[2],M.ASCE, T.H.C. Herbers[2], and P.F. Jessen[2]

ABSTRACT

The spectral evolution of swell propagating across a wide, shallow continental shelf is investigated with extensive data from the North Carolina shelf, on the East coast of the United States. A spectral energy balance equation is proposed for the evolution of swell that includes refraction and shoaling, bottom friction over a movable bed, and Bragg scattering of waves by wavelength-scale bottom topography. This equation is solved numerically using a hybrid Eulerian-Lagrangian model (Ardhuin et al., 2001). Hindcasts of swell events during recent field experiments show large variations in wave heights that can be attributed to refraction and bottom friction, and are consistent with a variable bottom roughness. Wave height attenuation up to 73 % (93 % of the wave energy) was observed in moderately energetic conditions. Bragg scattering of waves by wavelength-scale bottom features significantly increases (up to a factor two) the directional spread of waves.

INTRODUCTION

Many human activities in coastal areas require hindcasts or forecasts of the local wave climate. This information often relies on the transformation of wave conditions from the deep ocean to shallower water, using a wave model that must represent the interactions of waves with their environment: winds, currents, and bottom topography. In linear or quasi-linear models, waves must also change due to their mutual interaction to represent natural non-linear effects. Here we address part of this wave transformation problem by considering swell (long waves not significantly affected by the wind), in the absence of currents, well outside of the surf zone. We can therefore neglect deep-water non-linear effects (quartet wave-wave interactions) that have no significant effect on swell over the short propagation distances considered here, and shallow-water non-linear effects (triad wave-wave interactions) that are important only close to the surf zone. In these conditions, frequent along the exposed coastlines of the United States, the transformation of waves is essentially affected by the bottom

[1]Ingénieur de l'Armement, Centre Militaire d'Océanographie, Service Hydrographique et Océanographique de la Marine, BP 30316, 29609 Brest Cedex, FRANCE.

[2]Oceanography Department, Naval Postgraduate School, Monterey CA, 93943-5122

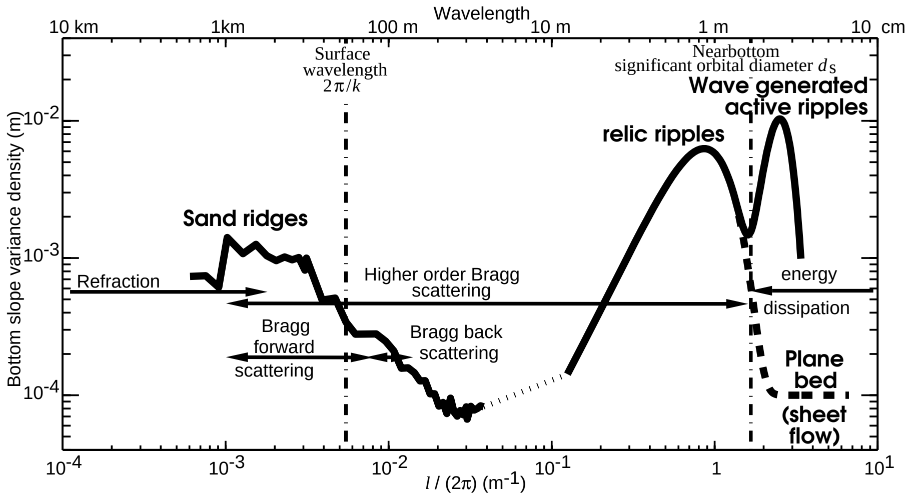

FIG. 1. Wave-bottom interactions, for different bottom horizontal scales (the bottom x-axis coordinate $2\pi/l$ is the reciprocal bottom wavelength). The thick curve is a typical bottom slope spectrum for the North Carolina shelf derived from bathymetry surveys for bottom wavelengths larger than 40 m. For small scales ($2\pi/l < 10$ m) the bottom topography depends on the wave conditions (solid curve: typical moderate swell, dashed curve: extremely large swells).

topography (Figure 1), and can be represented in a phase-averaged model, based on a spectral energy balance equation (Gelci, Cazalé & Vassal, 1957). Ardhuin and Herbers (2001) derived the energy balance equation for swell in a Lagrangian form, to which Ardhuin (2001) added bottom friction, to get

$$\frac{\mathrm{d}E\left(\mathbf{k}\right)}{\mathrm{d}t} = S_{\mathrm{Bragg}}\left(\mathbf{k}\right) + S_{\mathrm{fric}}\left(\mathbf{k}\right). \tag{1}$$

Wave refraction and shoaling over large-scale bottom features can induce large variations in wave energy along the coast. These effects are generally well understood, and accurately represented by linear refraction theory (e.g. Longuet-Higgins, 1957), and are included here in the left hand side of Eq. 1.

Medium scale (one half to several wavelengths) bottom features can change wave directions through a resonant wave-bottom interaction. This Bragg scattering process was first studied theoretically for random waves by Hasselmann (1966). At the lowest order in the surface and bottom slopes, two wave components with the same frequency but different wavenumber vectors $\mathbf{k}$ and $\mathbf{k}'$ exchange energy in a resonant triad interaction with the bottom component that has the difference wavenumber $\mathbf{l} = \mathbf{k} - \mathbf{k}'$. This phenomenon was first observed in the laboratory for regular waves over a sinusoidal topography by Heathershaw (1982), and higher order effects were measured by Belzons et al. (1991). Hasselmann's theory for random waves was corrected by Ardhuin and Herbers (2001), and shown to be valid for slowly varying wave and bottom elevation spectra. In Eq. 1 the lowest order Bragg scattering (class I) is represented in the right hand side by the source term S_{Bragg}. Ardhuin and Herbers (2001) showed that it could increase significantly the spread of narrow directional spectra.

Small-scale bottom features (smaller than the amplitude of the horizontal wave motion at the bottom) contribute to the roughness of the bottom and determine the dissipation of wave energy in the bottom boundary layer (Zhukovets, 1963). For seabeds composed of non-cohesive sandy sediments, these bedforms can be generated by the wave motion, taking the form of regular ripples, when the near-bottom wave velocity is strong enough to move sediments.

These processes have been investigated separately and in the laboratory. Their combination, represented by Eq. 1, is investigated here on the North Carolina continental shelf, in the wide and shallow region between Cape Hatteras and the entrance to the Chesapeake Bay, where effects of the bottom topography should be important, and where ripples were widely observed (Ardhuin et al., observations of wave-generated vortex ripples on the North Carolina continental shelf, 2001, submitted to *Journal of Geophysical Research*). The numerical wave model CREST (Ardhuin et al., 2001) is used to integrate Eq. 1 from the shelf break (using offshore wave observations) to the 8 m depth contour.

Model hindcasts over the two intensive field experiments DUCK94 and SHOWEX are compared with observations of wave evolution from two instrumented transects (Figure 2). Bottom-mounted pressure sensors, named A to I, were deployed across the shelf from August to December 1994 (DUCK94), giving wave frequency spectra every 3 hours (Herbers et al., 2000). Datawell Directional Waverider buoys, named X1 to X6, were employed from September to December 1999 (SHOWEX), providing frequency spectra every 30 minutes, and the first two Fourier components of the directional distribution. Additional wave measurements were provided by the National Data Buoy Center (NDBC), from 3-m pitch and roll discus buoy number 44014 and the infrared laser wave gauges mounted on C-MAN stations Diamond Shoals, DSLN7, and Chesapeake Lighthouse, CHLV2, and The US Army Corps of Engineers Field Research Facility (FRF), in Duck, North Carolina, from a coherent array of bottom pressure sensors, 8M, and a Waverider buoy, WR(FRF) (Figure 2, and Table 1).

CREST MODEL IMPLEMENTATION

CREST is a hybrid Eulerian-Lagrangian spectral wave model (Ardhuin et al., 2001), that uses an unstructured geographical grid. The spectral energy balance equation (Eq. 1) is a simple one-dimensional advection equation in its Lagrangian form. It is solved by advecting the **k**-space spectral densities of the wave energy along precomputed ray trajectories, from the model domain boundary to each point of the geographical grid. Ray trajectories are determined using a bathymetry grid with 6” resolution in latitude and longitude (180 and 150 m, respectively), generated from the National Ocean Service bathymetry database and depth soundings collected during DUCK94 and SHOWEX. The grid is smoothed for each frequency to remove bottom features with wavelengths larger than 4 times the local surface gravity wave wavelength. The ray integration is stopped at the boundaries between the nine subdomains (numbered 1 to 9 on figure 2), as described in Ardhuin et al. (2001). The precomputed ray trajectories are retained for subsequent use in time dependent source term computations.

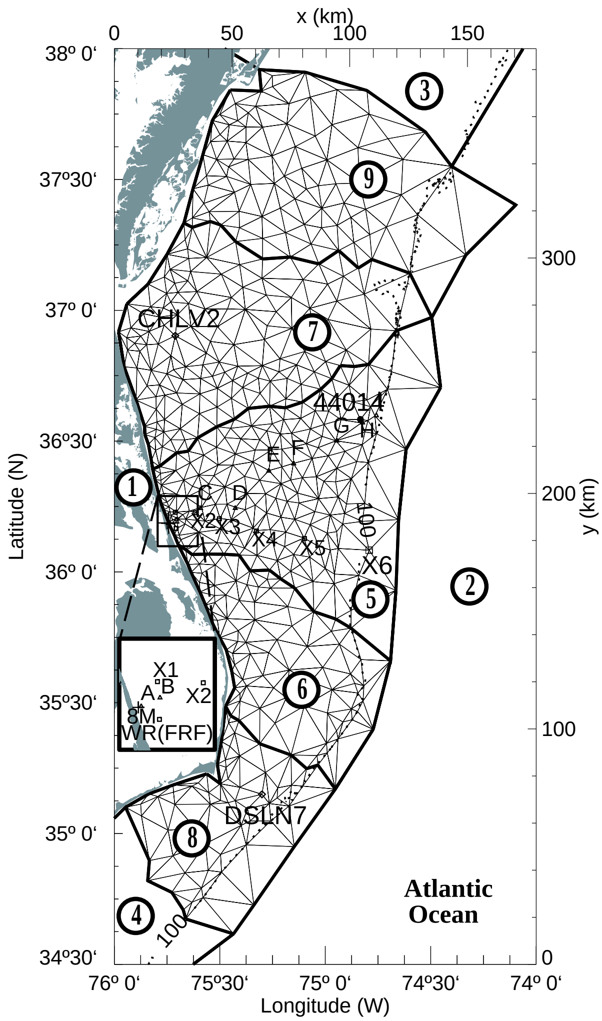

FIG. 2. Instrument locations during DUCK94 and SHOWEX. The 100 m depth contour is indicated by the dotted line, and the mesh represents the model grid. The grid points from which rays are computed and where the source terms are evaluated are the nodes of the triangular mesh. The entire model domain is divided into subdomains, numbered 1 through 9, separated by thicker lines.

Integration of the energy balance

The source terms in Eq. 1 are determined in Eulerian form from the spectrum at each grid point and interpolated in space and directions on the rays to give Lagrangian source terms. For each grid point Eq. 1 is averaged over finite bands of frequency (19 bands from 0.05 to 0.15 Hz) and arrival direction (72 bands, regularly spaced at 5 degrees intervals) and integrated in time using a first order Euler scheme with a fixed 10-minute time step. The wave-bottom Bragg scattering source term S_{Bragg} is estimated using a uniform bottom elevation spectrum determined from a 10 m resolution bathymetry grid of a 5 km $\times$ 5 km inner shelf region (Ardhuin and Herbers, 2001, figures 8b and 9a). The source term is computed for bottom wavelength less than 4

TABLE 1. Wave-measuring instruments during DUCK94 and SHOWEX. DUCK94 covers 1/8/1994 – 30/11/1994, and SHOWEX spans 13/9/1999 – 13/12/1999.

Name	water depth	directional	data availability	Operated by
8M	8.0 m	yes	02/1987 – present	FRF
WR(FRF)	17.0 m	no	10/80 – 11/96	FRF
WR(FRF)	17.0 m	yes	11/96 – present	FRF
44014	49 m	yes	10/90 – present	NDBC
CHLV2	15 m	no	9/84 – present	NDBC
DSLN7	18 m	no	11/88 – present	NDBC
A	12 m	no	DUCK94 until 17/11/94	NPS
B	21 m	no	DUCK94 until 17/11/94	NPS
C	26 m	no	DUCK94	NPS
D	34 m	no	DUCK94	NPS
E	35 m	no	DUCK94	NPS
F	33 m	no	DUCK94	NPS
G	46 m	no	DUCK94	NPS
H	49 m	no	DUCK94	NPS
I	87 m	no	DUCK94	NPS
X1	21 m	yes	SHOWEX	NPS
X2	24 m	yes	SHOWEX	NPS
X3	26 m	yes	SHOWEX	NPS
X4	33 m	yes	SHOWEX	NPS
X5	39 m	yes	SHOWEX	NPS
X6	193 m	yes	SHOWEX	NPS

times the surface wavelength, to separate the refraction and scattering scales.

The parameterization of bottom friction over a movable bed uses Shields numbers that are computed from the near-bed r.m.s. wave velocity, and the median grain size D_{50} of surficial sediments in the hindcast region. D_{50} for 50 surficial sediment samples (Ardhuin et al., submitted manuscript), and 20 core samples (Rebecca Beavers, Duke University, personal communication, 1999), varied between 0.09 and 4 mm. A spatially varying distribution of D_{50} is used here, although very similar results were obtained with a uniform value set to the median $D_{50} = 0.22$ mm. We generalize Tolman's (1994) decomposition of the bed roughness k_N in a ripple roughness k_r and sheet flow roughness k_s by taking

$$k_r = a_b \times A_1 \left(\frac{\psi}{\psi_c}\right)^{A_2} \frac{a_b^{-0.4}}{(2\pi)^2}, \tag{2}$$

where a_b and u_b are the r.m.s. amplitude of the bottom wave orbital displacement (half of the orbital diameter) and velocity at the top of the boundary layer, s is the sediment specific density, g is the gravity acceleration, ψ is the Shields number computed from u_b and D_{50} (Madsen et al., 1990), and ψ_c is its value at the onset of sediment motion. While Tolman (1994) used values of the empirical coefficients A_1 and A_2 determined by Madsen et al. (1990), we adjusted these coefficients to improve the present hindcasts of waves on the North Carolina shelf.

For ψ less than a critical value, ψ_{rr}, the bed roughness is given by a relic roughness k_{rr}, accounting for relic wave-generated bedforms and bioturbation. Madsen et al. (1990) proposed

$$\psi_{\mathrm{rr}} = A_3 \psi_c, \tag{3}$$

with $A_3 = 1.2$ determined empirically. Here the value of ψ_c, a function of the fluid and sediment physical properties, is taken from Soulsby (1997). Tolman (1994) proposed a constant value $k_{\mathrm{rr}} = 0.01$ m that yields good wave height predictions for very small waves. In order to represent the observed attenuation of larger waves we propose,

$$k_{\mathrm{rr}} = \max\{0.01\mathrm{m}, A_4 a_b\} \text{ for } \psi < \psi_{\mathrm{rr}}. \tag{4}$$

Parameter values $A_1 = 1.5$, $A_2 = -2.5$, $A_3 = 1.2$ and $A_4 = 0$ corresponds to Tolman's (1994) source term parameterization $S_{\mathrm{fric,T}}$. Here we propose $A_1 = 0.4$, $A_2 = -2.5$, $A_3 = 1.2$ and $A_4 = 0.05$, giving an improved source term $S_{\mathrm{fric,I}}$. A widely used alternative to this physics-based bottom friction source term assumes that S_{fric} is proportional to the bottom velocity spectrum, with a coefficient Γ/g^2. This 'JONSWAP' source term parameterization $S_{\mathrm{fric,J}}$ with $\Gamma = 0.038$ m^{2}s^{-3} is used here for reference.

Boundary conditions

The offshore frequency-direction wave spectra were estimated at X6 and 44014, with the Maximum Entropy Method (Lygre & Krogstad, 1986). After back-refracting the 44014 spectra to deep water, assuming parallel depth contours, 44014 and X6 spectra were interpolated to provide boundary conditions in domains 2 (offshore), 3 and 4 (north and south model limits). Time lags based on the deep water group speed of linear waves are applied between the boundary grid points and the measurement location (X6 and 44014) for each frequency-directional band. At the boundaries with domain 1 (land) a zero incoming flux was prescribed, corresponding to the absence of wave reflection from the beach and surf zone.

MODEL VALIDATION

Model results were compared with observations over swell-dominated time periods defined by the following criteria :

- a peak frequency f_p less than 0.12 Hz (reduced to 0.10 Hz for DUCK94, to avoid large depth correction errors at higher frequencies).
- a maximum wind speed less than 0.6 times the linear wave phase speed at the peak frequency $C(f_p)$, to exclude low-frequency wind-waves generated on the shelf in high wind conditions.

$C(f_p)$ is estimated from the Waverider buoy WR(FRF), on the inner shelf, and the wind speed is taken as the maximum of 1-hour averaged values $U_{19.5}$ measured at 19.5 m above sea level at the end of the FRF pier (close to the 8M array) and U_5 measured at 5 m above sea level on board buoy 44014. These conditions were verified for 528 hours (22 days) during SHOWEX and 363 (15 days) during DUCK94, out of the 87 days and 91 days of SHOWEX and DUCK94 observations, respectively.

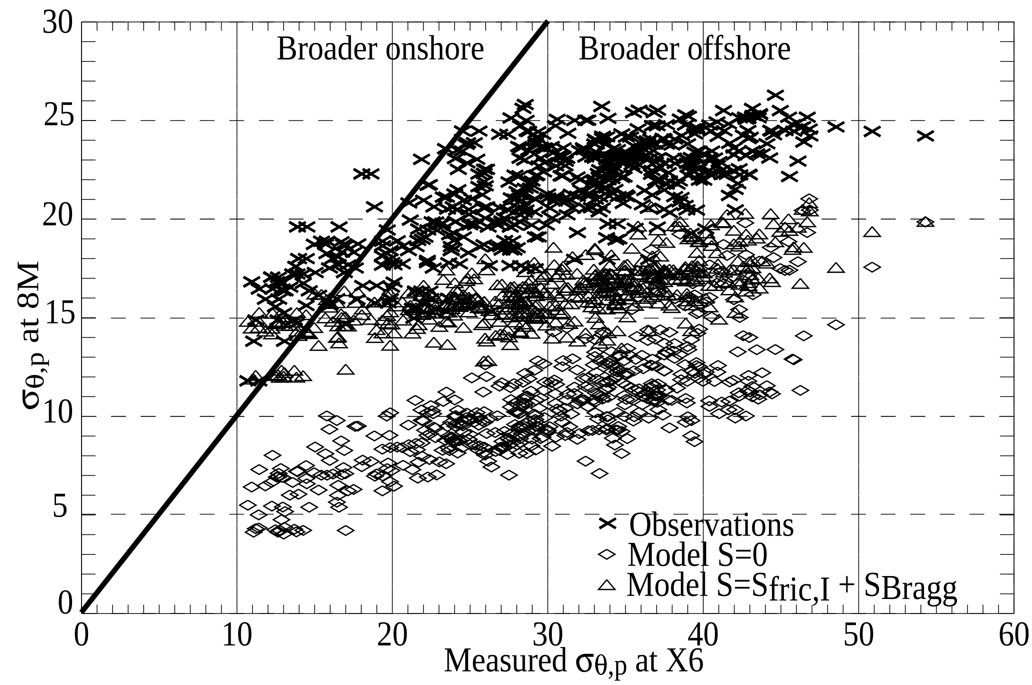

FIG. 3. Nearshore versus offshore directional spread $\sigma_{\theta,p}$, for all swell-dominated periods during SHOWEX. The solid line separates spectra that are broader in the nearshore and spectra that are broader offshore.

Wave directional properties

The evolution of wave directional properties across the shelf was measured during SHOWEX only. In the model they are influenced primarily by refraction, that modifies the mean wave direction, and Bragg scattering that increases the directional spread. A mean direction θ_p at the peak frequency f_p was computed for each instrument, from the first Fourier coefficients of the directional distribution, using an energy-weighted average over a finite bandwidth of $0.15 f_p$ centered at f_p. f_p was determined from the measured frequency spectra at X1, so that the modeled and observed directions correspond to the exact same frequency band. θ_p is well predicted by the model with no source terms or bottom friction only, with a maximum root mean square (r.m.s.) error of 8–10 degrees on the inner shelf, that decreases onshore as refraction narrows the incoming spectra toward the beach-normal direction of 70° (not shown).

The directional spread at the peak frequency $\sigma_{\theta,p}$ was defined along the same lines, using the definition of Kuik et al. (1988). Observed values of $\sigma_{\theta,p}$ are generally stable across the shelf and slightly decrease close to the shore (figure 3, crosses). However, whenever the offshore directional spectrum is very narrow ($\sigma_{\theta,p}(X6) < 20°$), $\sigma_{\theta,p}$ increases towards the shore. This observation is contrary to the general belief that wave fields become directionally narrow in shallow water, owing to depth-refraction. Model calculations that incorporate refraction, as well as bottom friction (in order to provide reasonable wave heights) give directional spreads much narrower than the observations (figure 3, diamonds). This bias, largest at 8M and on the inner shelf, can be observed

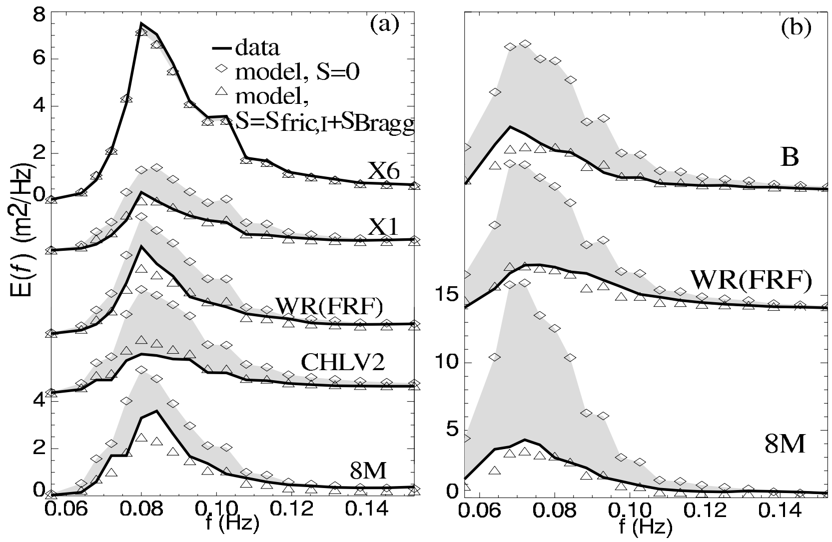

FIG. 4. Observed and predicted wave frequency spectra averaged over 12 hours for easterly waves and (a) moderate offshore wave heights (2 m, 18 November 1999) and (b) larger offshore waves (2.8 m, 19 October 1994). The shaded areas represent the wave energy dissipated between offshore and the local position (difference between observations and model runs without source terms).

throughout the shelf. The addition of Bragg scattering in the energy balance (Eq. 1) dramatically increases $\sigma_{\theta,p}$, and yields a better agreement with observations (figure 3, triangles).

Wave attenuation across the shelf

Changes in the peak frequency across the shelf are small, but wave energy may be strongly attenuated. This wave height reduction is explained only in part by refraction of waves that propagate onshore at large oblique angles to the depth contours. For the case shown in figure 4a the wave attenuation from X6 (offshore) to 8M (in 8 m depth) is equally due to refraction and bottom friction. In figure 4b refraction is negligible and the strong attenuation of these larger waves can be explained by bottom friction alone, in this case active sand ripple formation is expected over most of the shelf (Ardhuin et al., 2001).

Over all swell-dominated conditions observed during DUCK94 and SHOWEX, the model with only refraction and shoaling overpredicts wave heights with a typical bias of 0.2 m on the inner shelf, and gives an overall (for all sensors) scatter index (ratio of r.m.s. error and r.m.s. value) of 0.26 for H_s (figure 5). Adding Bragg scattering slightly increases model errors. Indeed an increased directional spread translates into a larger cross-shelf propagation time (on average), which, in the absence of dissipation, increases the wave height, giving an overall scatter index of 0.29.

Including bottom friction dramatically reduces model errors. Tolman's (1994) movable-bed source term, based on laboratory data without any empirical tuning to field conditions, mimics the observed variable attenuation of waves, and yields a re-

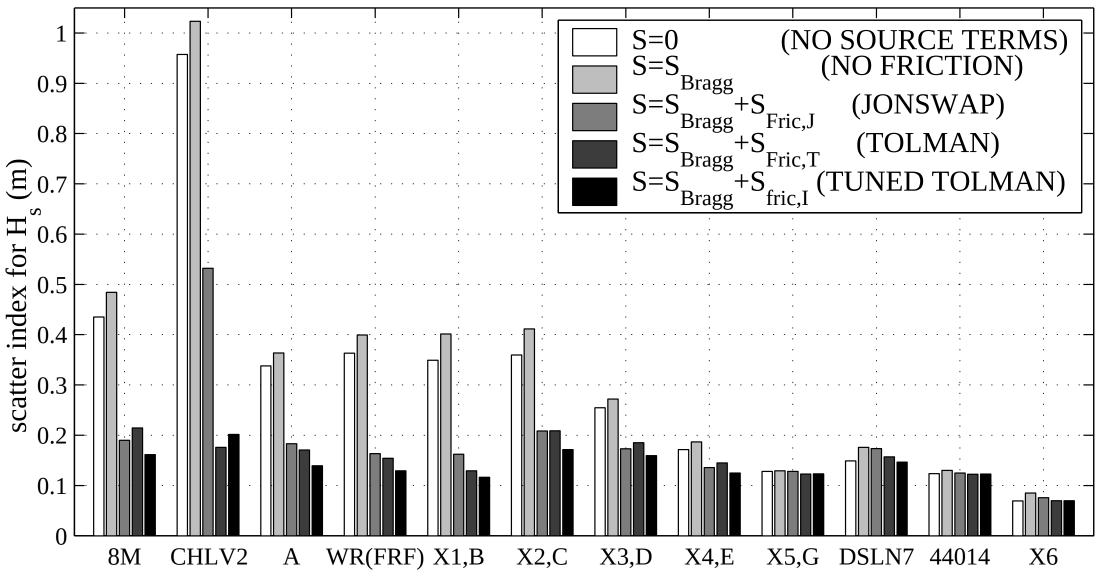

FIG. 5. Scatter index for predictions of the significant wave heights H_s, in swell-dominated periods observed during SHOWEX and DUCK94, for different sets of source terms. Data from closely located instrumented sites during DUCK94 and SHOWEX have been grouped (e.g. X1 and B).

duced overall scatter index of 0.15. This result supports the hypothesis that the formation of vortex ripples and their feedback on the waves through enhanced bottom roughness, are the primary mechanisms for wave attenuation across a sandy continental shelf. On average the empirical JONSWAP bottom friction source term performs about equally well (figure 5), with an overall scatter index of 0.16. However, this source term gives poor results at CHLV2, a site located down wave of shallow shoals (but not shallow enough for depth-induced breaking), with a scatter index of 0.53 and a positive bias of 20 cm. This bias is the result of large model-data discrepancies during the arrival of swell from Hurricane Gert (17–21 September 1999). Observed wave heights at CHLV2 during this event are 73% smaller than predicted by refraction and shoaling, which corresponds to a dissipation of 93% of the incident wave energy flux. This is probably the result of active ripple generation on the shoals offshore of CHLV2, and the JONSWAP source term is known to largely underpredict bottom friction over active ripples (Ardhuin et al., 2001). Our 'tuned Tolman source term' $S_{\mathrm{fric,I}}$ gives an overall scatter index of 0.13.

CONCLUSION

The numerical wave model CREST was implemented on a large portion of the North Carolina–Virginia continental shelf for a comprehensive hindcast of all swell-dominated conditions observed during the experiments DUCK94 and SHOWEX. Bragg scattering over the small-scale (comparable to the surface wavelength) shelf topography explains most of the observed broadening of the wave spectrum towards the shore, that occasionally balances the narrowing caused by refraction over the quasi-plane large-scale bathymetry. The variable attenuation of large swells (inferred dissipation up to 93% of the incident wave energy flux) is well reproduced by Tolman's (1994) bottom friction source term, that accounts for the generation of sand ripples by waves and their feedback on the waves. The energy balance equation (Eq. 1), with movable-bed bottom friction and wave-bottom Bragg scattering source terms, provides a good description of spectral swell dissipation and directional spreading across the North Carolina continental shelf, improving on previous physics-based models.

ACKNOWLEDGMENTS

We are grateful to R. Jensen and R. Long (USACE) and NDBC for providing wave data, T. Stanton, F. Dobson and M. Donelan, for multibeam bathymetry surveys, and M. Orzech for generating the bathymetry grid.

REFERENCES

Ardhuin, F. (2001). "Swell across the continental shelf," PhD thesis, Naval Postgraduate School. [http://www.oc.nps.navy.mil/˜ ardhuin/index.html].

Ardhuin, F., Drake, T. G., and Herbers, T. H. C. (2001). "Observations of wave-generated vortex ripples on the North Carolina continental shelf." *J. Geophys. Res.* submitted manuscript.

Ardhuin, F. and Herbers, T. H. C. (2001). "Bragg scattering of random surface gravity waves by irregular sea bed topography." *J. Fluid Mech.* In press.

Ardhuin, F., Herbers, T. H. C., and O'Reilly, W. C. (2001). "A hybrid Eulerian-Lagrangian model for spectral wave evolution with application to bottom friction on the continental shelf." *J. Phys. Oceanogr.*, 31(6), 1498–1516.

Belzons, M., Rey, V., and Guazzelli, E. (1991). "Subharmonic bragg resonance for surface water waves." *Europhysics Letters*, 16(2), 189–194.

Gelci, R., Cazalé, H., and Vassal, J. (1957). "Prévision de la houle. la méthode des densités spectroangulaires." *Bulletin d'information du Comité central d'Océanographie et d'Etude des Côtes*, 9, 416–435.

Hasselmann, K. (1966). "Feynman diagrams and interaction rules of wave-wave scattering processes." *Review of Geophysics*, 4(1), 1–32.

Heathershaw, A. D. (1982). "Seabed-wave resonance and sand bar growth." *Nature*, 296, 343–345.

Herbers, T. H. C., Hendrickson, E. J., and O'Reilly, W. C. (2000). "Propagation of swell across a wide continental shelf." *J. Geophys. Res.*, 105(C8), 19,729–19,737.

Kuik, A. J., van Vledder, G. P., and Holthuijsen, L. H. (1988). "A method for the routine analysis of pitch-and-roll buoy wave data." *J. Phys. Oceanogr.*, 18, 1020–1034.

Madsen, O. S., Mathisen, P. P., and Rosengaus, M. M. (1990). "Movable bed friction factors for spectral waves." *Proceedings of the 22nd international conference on coastal engineering*, ASCE. 420–429.

Soulsby, R. (1997). *Dynamics of marine sands, a manual for practical applications*. Thomas Telford Publications, London.

Zhukovets, A. M. (1963). "The influence of bottom roughness on wave motion in a shallow body of water." *Izv. Acad. Sci. USSR Geophys. Ser.*, 10, 1561–1570.

KEYWORDS FOR
'SPECTRAL EVOLUTION OF SWELL ACROSS THE CONTINENTAL SHELF'

waves
swell
bottom friction
Bragg scattering
sand ripples
Duck
CREST
rays
modeling
SHOWEX